Functional Materials Letters
Vol. 10, No. 3 (2017) 1750014 (4 pages)
© World Scientific Publishing Company
DOI: 10.1142/S179360471750014X

World Scientific
www.worldscientific.com

Funct. Mater. Lett. 2017.10. Downloaded from www.worldscientific.com
by NATIONAL AUTONOMOUS UNIVERSITY OF MEXICO (UNAM) on 04/25/18. For personal use only.

Size distribution and visible luminescence of silicon nanoparticles embedded in SiN_x thin film: Role of RF power in PECVD

Luis Andres Gómez-González*, Ateet Dutt*, Betsabee Marel Monroy*,
Juan David Escobar-Carrasquilla* and Guillermo Santana*,§
*Instituto de Investigaciones en Materiales
Universidad Nacional Autónoma de México, CD. Universitaria A.P. 70-360
Coyoacán, C.P. 04510, México, D.F

Carlos Álvarez-Macías† and Arturo Ponce‡
†Departamento de Ingeniería de Procesos e Hidráulica
Universidad Autónoma Metropolitana
Iztapalapa, A.P. 55-534, 09340, México, D.F

‡Department of Physics and Astronomy, The University of Texas at San Antonio
San Antonio, Texas 78249, USA
§gsantana@iim.unam.mx

Received 17 August 2016; Accepted 29 November 2016; Published 13 January 2017

This paper presents, the studies of the influence of (radio frequency) RF power on the size distribution and visible photoluminescence (PL) of SiN_x thin film deposited at 300°C of substrate temperature by plasma enhanced chemical vapor deposition. RF power was varied (5–50 W), and its aftereffect on the optical properties of thin films was investigated. By increasing the RF power between 5 W and 25 W, main PL peak showed a red shift with an increase in PL intensity, which is associated with an increase in the silicon nanocrystals size and density, respectively. Results obtained were confirmed with High-resolution transmission electron microscopy micrographs and from the statistical calculations. By attaining a precise RF power value, stable silicon nitride thin film with suitable optical properties can be achieved for the potential fabrication of optoelectronic devices.

Keywords: Chemical vapor deposition; nanoparticles; electron microscopy; photoluminescence; FTIR.

Silicon is the most important semiconductor in the microelectronic and photovoltaic industries.[1–3] Reasons are as follows: it is the second most abundant element on the surface of the Earth, and it has very good optical, electrical and mechanical properties. On the other hand, crystalline silicon (c-Si) has a small (1.12 eV) and indirect band gap[4,5] and therefore, the electron-hole recombination after excitation is nonradiative, and the inefficient radiative recombination is in the infrared (IR) region.[5] To obtain stable and passivated silicon nanoparticles, it is important that they are embedded in matrices like silicon oxide (SiO_x), silicon nitride (SiN_x) silicon carbide (SiC) and silicon oxy-carbide.[6–9]

Silicon nitride (Si_3N_4) is a wide band-gap semiconductor, and it has attracted much attention for the optical as well as its suitable mechanical properties.[10] Also, previous studies related to Si_3N_4 show that the photoluminescence (PL) properties mainly originated from surface defects.[11] Until now, numerous investigations have been put forward to develop Si_3N_4 thin films with emission in the visible region using plasma enhanced chemical vapor deposition (PECVD) equipment.[12–15]

Even in the earlier reports, detailed description of the formation of silicon nanoparticles in the size regime (2–4 nm) via nucleation mechanism by means of PECVD has been presented.[16] Among various published reports, one of them was focused on the radio frequency (RF) power variation in PECVD and in the same article, luminescence was related to the defect sites.[17] On the other hand, in one of the recent reports, role of defect states using a bit high RF power (in comparison to present work) on the luminescence has been shown.[18]

In this paper, foremost, intensive research has been made for finding the role of RF potential on the structural as well as the optical property of silicon thin films deposited by PECVD. Apart from using one of the most commonly used

§Corresponding author.

precursors (silane) for attaining Si_3N_4 thin films,[19] in the present work, unique precursor (dichlorosilane) is used. Dichlorosilane is a very significant precursor material as its reactivity (surface chemistry) provokes the formation of silicon nanocrystals at room temperature without the need of annealing treatments. Influence of the dichlorosilane chemistry on the formation of Si nanoparticles (structural properties) has been discussed earlier in one of our studies.[20] Moreover, in one of our recent reports, a very detailed description of the formation of Si quantum dots (silicon or nitrogen rich environment) in the PECVD system along with the theoretical simulations has been presented.[21]

Finally, in the present work, a brief explanation is given for the mechanism of bright visible emission from the silicon thin films at room temperature and prospects for future device fabrication is presented.

The nc-Si/SiN_x was deposited by PECVD using a conventional radio frequency (13.56 MHz), parallel-plate (150 cm^2 in area, 1.5 cm apart) system. The films were deposited on fused silica and (1 0 0) n-silicon high resistivity substrates for their optical and structural characterization, respectively. High purity gases were used with different mass flows rates: 40 sccm of H_2, 50 sccm of Ar, 5 sccm of SiH_2Cl_2 and 25 sccm of NH_3. The RF power was varied from 5 W to 50 W at a fixed pressure of 500 mTorr. For the structural characterization, high-resolution transmission electron microscopy (HRTEM) was carried out in a field emission gun microscope (FEI-TITAN 80–300 kV) which operates at 300 kV. The bonding structure of the films was analyzed using a Fourier Transform Infrared (FTIR) spectrometer (Nicolet-540). PL studies were carried out at room temperature using He-Cd laser ($\lambda = 325$ nm) at 16 mW.

Figure 1(a) shows the absorption spectra obtained for fresh samples grown by varying the RF power. All of the spectra showed an absorption band associated with Si-N bonds (stretching vibration mode) at 896 cm^{-1}, thus, confirming the presence of a Si_2N_4 matrix. The peak situated at $\sim$2200 cm^{-1} is related to Si-H bonds in its stretching vibration mode, while the peak located at $\sim$3365 cm^{-1} is related to N-H bonds in its mode of vibration stretching. From FTIR spectra, one can quantify the hydrogen content of which is bonded with Si and N in Si_3N_4 films. To calculate the concentrations of Si–H and N–H two equations were used, respectively.[22]

From Fig. 1(b), it can be illustrated that for the particular intermediate RF power from 20 W to 30 W, deposited films show almost same kind of bond concentration for Si–H and N–H bonding. This property clearly remarks the chemical stability of material at these particular potential values.

To go profound with the microstructural investigation, HRTEM study was made for the sample deposited at 25 W and 30 W.

Figure 2(a) shows the HRTEM micrograph for the sample grown at 25 W, whereas, inset is showing the Fourier transform of one of the selected region. After carrying out more statistical studies on the HRTEM image, it is found that the average size of nanoparticles is 1.7 nm with a standard deviation of 0.44 nm and density of nanoparticles is around 3.5×10^{12} nc/cm^2, Fig. 2(b).

Figure 3(a) shows the HRTEM image of the film grown at statical calculations. In this case, statistical analysis gave the average size of 3.5 nm with a standard deviation of 0.83 nm and an average density of 6×10^{12} nc/cm^2.

Figure 4 shows a graph representing the behavior of these films following the Tauc's model for the sample grown at

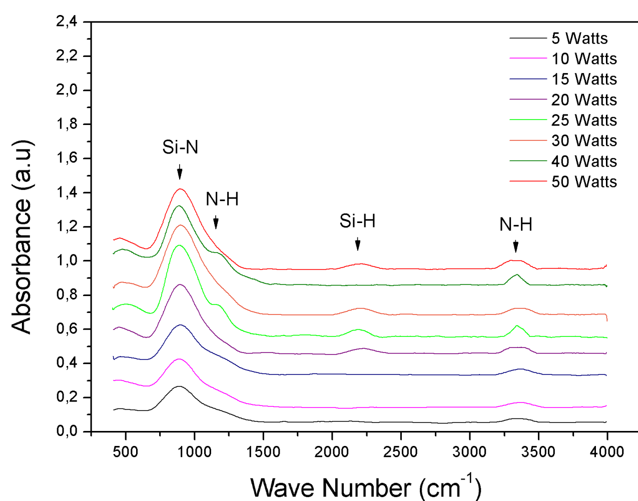

(a)

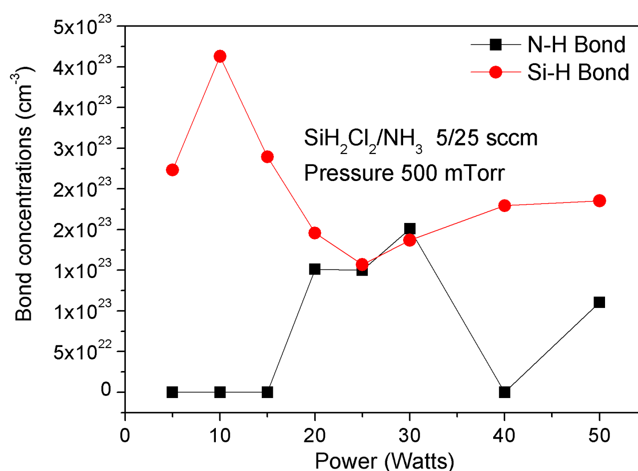

(b)

Fig. 1. (a) FTIR absorption spectra and (b) concentration of hydrogen bonds as a function of RF powers.

Funct. Mater. Lett. 2017.10. Downloaded from www.worldscientific.com by NATIONAL AUTONOMOUS UNIVERSITY OF MEXICO (UNAM) on 04/25/18. For personal use only.

Funct. Mater. Lett. 2017.10. Downloaded from www.worldscientific.com
by NATIONAL AUTONOMOUS UNIVERSITY OF MEXICO (UNAM) on 04/25/18. For personal use only.

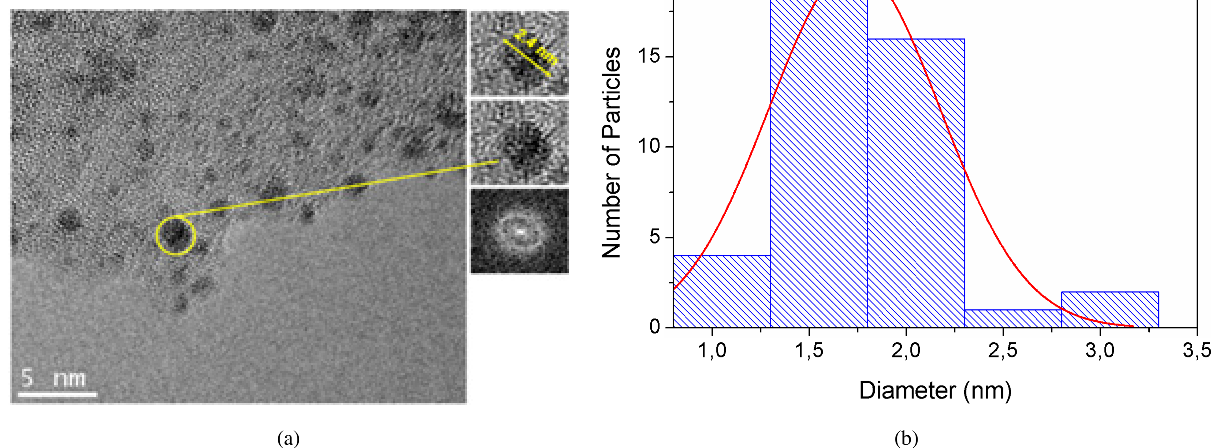

Fig. 2. (a) HRTEM image of silicon nanocrystals grown at 25 W and 500 mTorr. (b) Image size distribution of silicon nanocrystals.

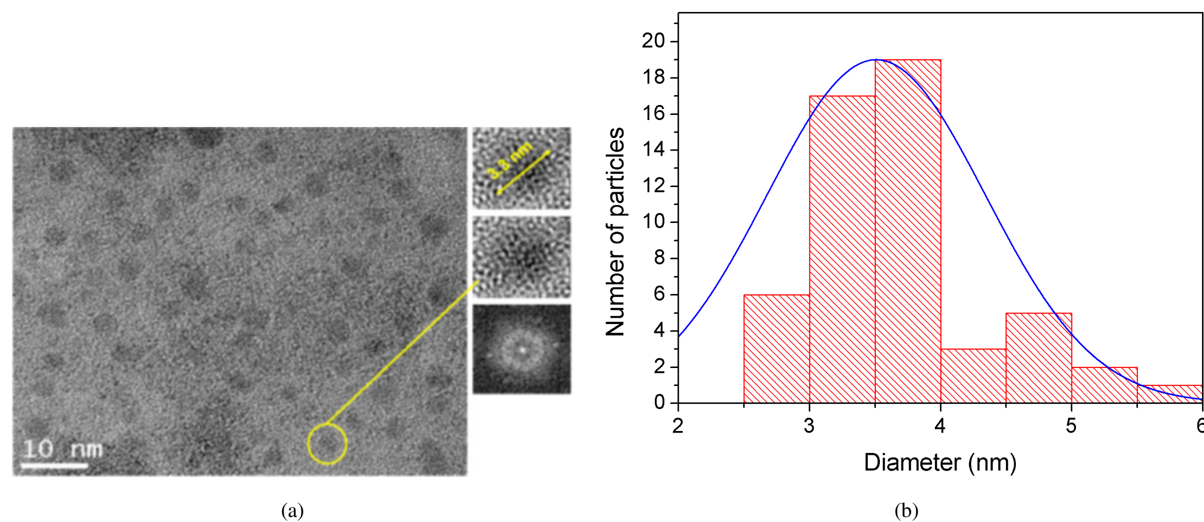

Fig. 3. (a) HRTEM image of silicon nanocrystals inside the SiN_x film grown at 30 W power. (b) Diameter distribution of silicon nanocrystals.

30 W. From this graph, it can be seen that the optical band gap of the sample is located at 4.19 eV. This is a direct measurement of the effective gap of our material.

After carrying out the structural analysis and determining the size distribution, and the band gap of the thin films, a more optical study was conducted of the samples deposited at RF power of 25 W and 30 W.

Figure 5 shows the PL of the sample when excited with a laser of 325 nm (He–Cd), whereas inset shows the real color emission from the sample. In general, sample exhibited a broad spectrum from 380 nm to around 700 nm with broad shoulders appearing at 380 nm, 450 nm, the peak intensity at 514.21 nm and another peak at around 600 nm. From Figs. 2(a) and 2(b), it is clear that in the case of sample deposited at 25 W the average size is around 1.7 nm and density is around 3.5×10^{12} nc/cm^2, whereas in the case of

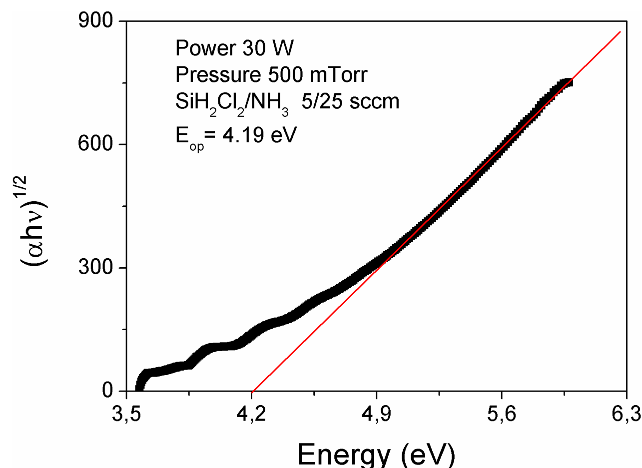

Fig. 4. Tauc's graph corresponding to the sample grown at an RF power of 30 W and pressure of 500 mTorr.

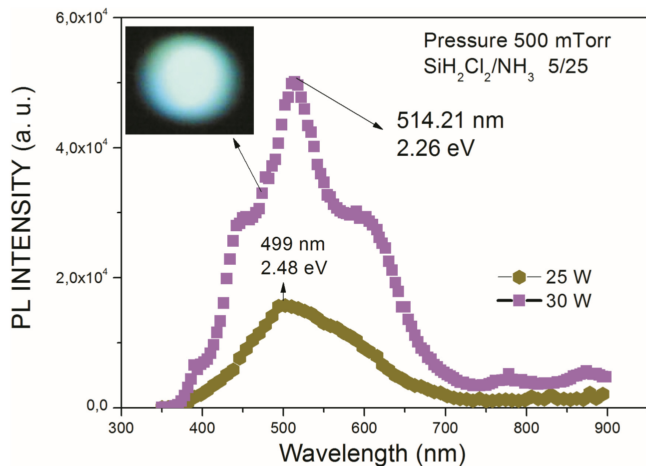

Fig. 5. Room temperature PL spectra for the sample grown at 25 W and 30 W when excited with 325 nm laser source. Inset is showing the real color emission from the sample in ambient conditions with the naked eye.

30 W size is around 3.5 nm and density is 6×10^{12} nc/cm^2. Difference in the size as well as in density distribution of two respective RF powers explains the shift and dissimilarity in the intensity of PL peaks. Sample deposited at 30 W has higher density size of large sized nanoparticles. It could provoke the shift in the PL peak to lower energy (higher wavelength) with more intensity. However, for the sample deposited at 25 W, lower size, as well as density, caused the blue shift with less luminescence intensity. All of the results revealed here shown good concordance with the quantum confinement effect proposed by Kim *et al.*, in previous reports. Results obtained in the present case show that the main origin of luminescence is from the quantum confinement effect in silicon nanocrystals embedded in Si_3N_4 matrix.

In conclusion, in this paper, the role of RF power is demonstrated for attaining stable and highly luminescent thin films. By increasing the power between 5 W and 50 W, it was observed that films at 25 W and 30 W were more chemically stable. Structural and optical studies were made for these two respective power values. Film deposited at 25 W show a shift in the position of the PL main peak from green to blue. It is related to the average size of nc-Si embedded in the nitride matrix. At higher RF power, i.e. 30 W, the main PL peak position shifts to green region. For this particular sample, the size and density of silicon nanocrystals were almost double as compared to the other sample. This increases the PL intensity, which is associated with higher density of silicon nanocrystals and better passivation. Results obtained in this paper show that the PL is from the quantum confinement effect in silicon nanocrystals. Present study shows a particular RF power which could be used for the fabrication of stable and highly luminescent thin films, which could be used for the fabrication of optoelectronic devices.

Acknowledgments

The Authors acknowledge the financial support from CONACyT doctoral scholarships (CVU 255507 and CVU 445952). A. Dutt also acknowledges the post-doctoral scholarship from UNAM (CVU 462696). Financial support for this work is from DGAPA-UNAM PAPIIT Project IN108215. Also, authors are indebted to Adriana Tejeda, Josué Esau Romero Ibarra and Carlos Ramos Vilchis, for their technical support.

References

1. S. M. Sze, *Semiconductor Devices: Physics and Technology,* 2nd edn. (Johon Wiley & Sons, New York, 1995).
2. V. Filip *et al.*, *25th Int. Conf. Microelectronics* (2006), pp. 261–267.
3. T. Saga, *NPG Asia Materials* **2**, 96 (2010).
4. L. M. Cohen *et al.*, *Phys. Rev.* **141**, 789 (1966).
5. S. S. Iyer *et al.*, *Science* **260**, 40 (1993).
6. R. Smirani *et al.*, *J. Lumin.* **115**, 62 (2005).
7. Li Wang *et al.*, *Solid State Commun.* **117**, 239 (2001).
8. A. Dutt *et al.*, *Mate. Lett.* **131**, 295 (2014).
9. I. Stenger *et al.*, *Appl. Phys Lett.* **92**, 241114 (2008).
10. W. Y. Yang *et al.*, *J. Phys. Chem. B* **111**, 4156 (2007).
11. G. F. Zou *et al.*, *Appl. Phys Lett.* **86**, 181901 (2005).
12. H. Du *et al.*, *Mat. Lett.* **84**, 31 (2012).
13. Y. Xin *et al.*, *Thin Solid Films* **516**, 1130 (2008).
14. M. Anutgan *et al.*, *J. Lumin.* **131**, 1305 (2011).
15. D. H. Ma *et al.*, *Superlattices Microstruct.* **93**, 269 (2016).
16. L. Boufendi *et al.*, *J. Phys. D: Appl. Phys.* **44**, 1 (2011).
17. S. Jang *et al.*, *J. Alloys Compd.* **614**, 102 (2014).
18. S. Jang *et al.*, *RSC Adv.* **6**, 88229 (2016).
19. B. Barwe *et al.*, *J. Phys. D: Appl. Phys.* **48**, 1 (2015).
20. A. Remolina *et al.*, *Phys. Status Solidi C* **8**, 850 (2011).
21. E. Mon-Pérez *et al.*, *Nanotechnology* **27**, 1 (2016).
22. G. Santana *et al.*, *J. Non. Cryst. Solids* **351**, 922 (2005).
23. T. Y. Kim *et al.*, *Appl. Phys Lett.* **85**, 5355 (2004).

Funct. Mater. Lett. 2017.10. Downloaded from www.worldscientific.com by NATIONAL AUTONOMOUS UNIVERSITY OF MEXICO (UNAM) on 04/25/18. For personal use only.